# Analysis of Iron and Copper Production Activity in Central Anatolia during the Assyrian Colony Period

*Hideo AKANUMA*
*Iwate*

## 1. INTRODUCTION

In 1994, three iron fragments were found in architectural remains dating to the Assyrian Colony Period (20th to 18th c. B.C.) at the site of Kaman-Kalehöyük, Turkey. Archaeometallurgical analyses have revealed that two of the fragments have the composition of steel (Akanuma 2002; 2003). In addition, it was determined that two fragments excavated from the Karum Ib level (19th to 18th c. B.C.) at the site of Kültepe in central eastern Anatolia were made of artificially produced iron (Akanuma 2003). Furthermore, another iron fragment made of steel was discovered in structures dating to the Old Hittite Kingdom Period (18th to 14th c. B.C.) at Kaman-Kalehöyük (Akanuma 2003). It is generally believed that the transition from bronze to iron in the Near East occurred through the diffusion of Hittite Empire iron production technology after the downfall of the Hittite Empire. However, these archaeometallurgical results strongly suggest that a steel production method had already been established before the birth of the Hittite Empire.

After the archaeometallurgical analyses of the above-mentioned six iron fragments, two more iron objects discovered at Kaman-Kalehöyük in 1992 and 1994 were excavated from structures believed to date to the Assyrian Colony Period. [1)] One of them was iron slag. Moreover, a small copper lump and three lumps of copper slag were also found in other Assyrian Colony Period structures in 1992 and 2006, respectively. Based on these recent excavation finds and archaeometallurgical results, we can surmise that some kind of production activity related to iron and copper occurred at Kaman-Kalehöyük during the Assyrian Colony Period.

This paper examines the archaeometallurgical results of five iron objects and four copper objects from Kaman-Kalehöyük dating to the Assyrian Colony Period. It then examines the production and exchange of iron and copper materials in the Kaman-Kalehöyük region during this period.

## 2. OBJECTS ANALYZED

Eight objects excavated from Stratum IIIc (the Assyrian Colony Period) and one object from Stratum IIIb-IIIc at Kaman-Kalehöyük were examined (Samples No.1 through No.9). Samples No.2, No.3, and No.4 (Fig. $1a_1$) are small iron fragments excavated from the architectural remains called Room 150 (Akanuma 2002; 2003). Sample No.1 (Fig. $1a_1$) is a small iron fragment and Sample No.5 (Fig. $2a_1$) is a blackish-brown lump of iron slag that also contains iron corrosion products. Samples No.1 and No.5 were considered to belong to a structure dating to the Old Hittite Empire Period (IIIb) and the cultural age of Stratum III, respectively (Akanuma 1995a; 1995b).Recently, the attribution of Samples No.1 and No.5 were reexamined by Dr. Sachihiro Omura and his co-workers; their research placed the samples in Stratum IIIc. Samples No.1 to No.5 were previously analyzed and reported (Akanuma 1995a; 1995b; 2002; 2003; 2005); the chemical composition and the microstructure of Sample No.5 were reanalyzed for this paper. In addition, in order to take into account the influence of contamination from burial deposits, subsamples extracted from the surface of four iron fragments on whose surfaces a lot of soil remained (Samples No.1 to No.4) were analyzed again.

---

[1)] Dates of these two iron objects were determined by Dr.Sachihiro Omura and Dr. Kimiyoshi Matsumura.

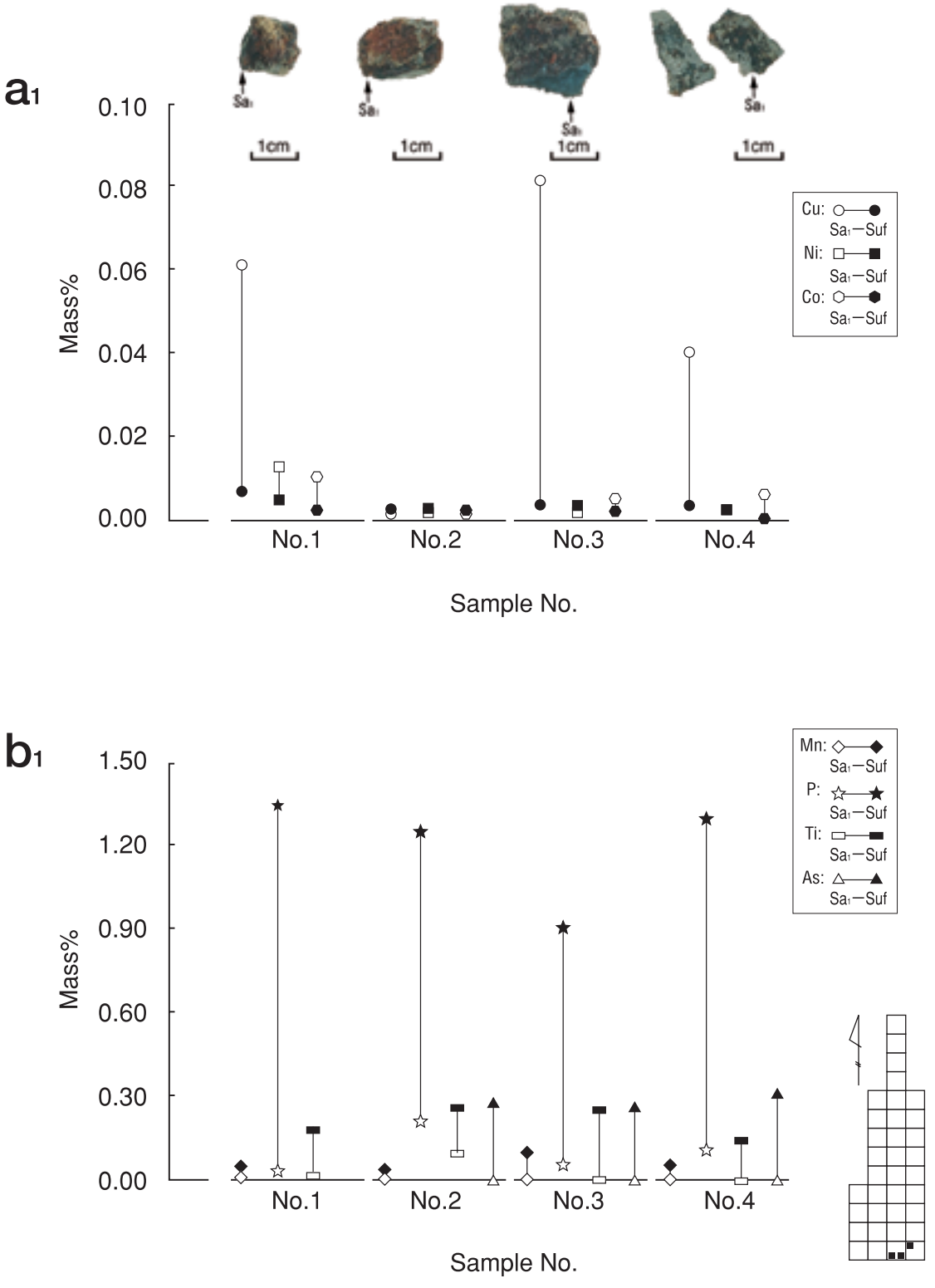


Fig. 1. Comparison of the chemical composition between the inner samples ($Sa_1$) and the surface samples (Suf) extracted from iron artifacts Samples No.1 through No. 4 from Stratum IIIc. $a_1$: Comparison of the Cu, Ni, and Co contents. $b_1$: Comparison of the Mn, P, Ti, and As contents.

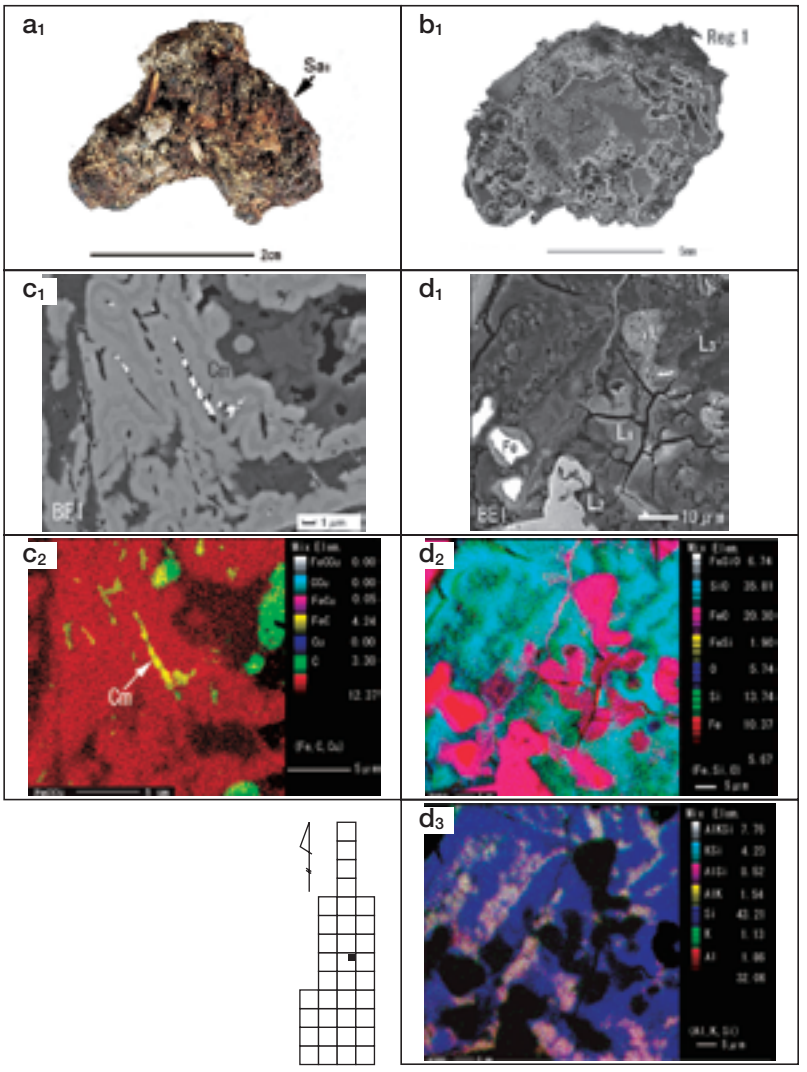


Fig. 2. Metallographic analysis of Sample No.5 excavated from Stratum IIIc. $a_1$: External appearance. The metallographic sample was extracted from the marked location. $b_1$: Macrostructure. $c_1$ and $c_2$: Backscattered electron (BE) image and a combined X-ray color-map of Fe-Kα, C-Kα and Cu-Kα within the area (Reg.1) in $b_1$. Cm: Cementite or its holes. $d_1$ to $d_3$: BE image and combined X-ray color-maps of Fe-Kα, Si-Kα, and O-Kα, and Al-Kα, K-Kα, and Si-Kα within the area (Reg.1) in $b_1$ ($d_1$ is adjacent to $c_1$ in the area (Reg.1) in $b_1$). (Excavation plan from Omura 2005)

Sample No.6 (Fig. 3$a_1$) is a small copper lump and Samples No.7, No.8, and No.9 (Figs. 4$a_1$, 5$a_1$, and 6$a_1$) are copper slag whose color is dark brown.

Table 1 lists the archaeological provenience data for each object.

## 3. SAMPLE PREPARATION

The following subsamples were taken from each artifact: approximately 20-30 mg from the surface of each of the four iron artifacts (Nos. 1 through 4), approximately 200 mg from the inner portion of the lump of iron slag (No.5), and approximately 0.5 to 1g from the copper lump (No.6) and three lumps of copper slag (Nos. 7 through 9). Sampling was performed using a portable drill equipped with a diamond cutting wheel. Surface subsamples, indicated by "Suf" in Table 2, were composed mainly of soil and a small amount of corrosion products; inner subsamples are indicated by "$Sa_1$" in Table 2. The analysis of each inner subsample from Samples No.1 to No.4 was performed between 1995 and 2003 (Akanuma 1995a; 1995b; 2002; 2003). Sample No.5 was sampled and analyzed again, adding As and S content; see Table 3, where the designation "(n)" is given to the new data.

Each subsample taken from the copper objects (Nos. 6 through 9) was divided into two parts: the larger part was used for metallographic observation, and the smaller part was used for chemical analysis.

## 4. ANALYTICAL METHODS

The samples to be used for metallographic observation (subsamples from No.1 and from Nos.5 through 9) were sectioned, mounted with epoxy resin, ground with emery paper, and then polished using diamond paste. The prepared samples were then examined under an optical microscope. Electron microprobe analyses (EPMA) were then performed with a JEOL JXA 8100 equipped with three wavelength-dispersing X-ray spectrometers, in order to examine the microstructure and to identify the metal and mineral phase compositions in the iron slag,

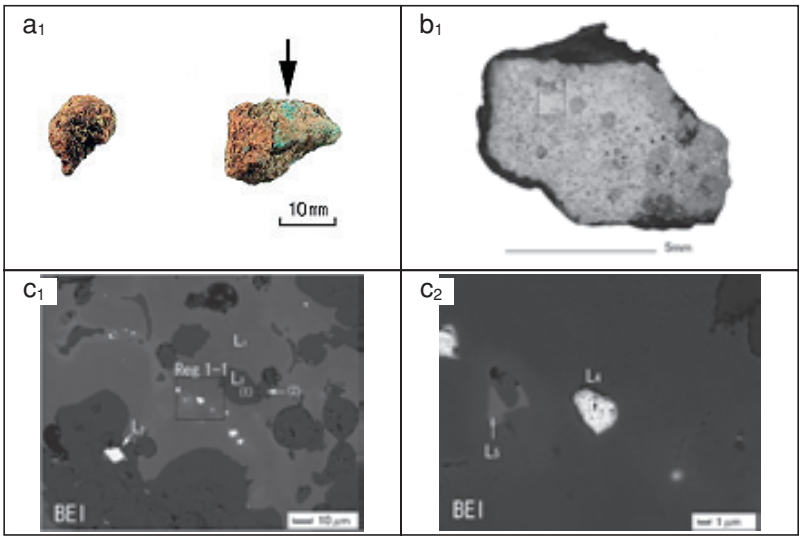


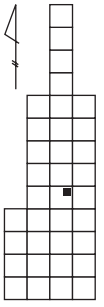

Fig. 3. Metallographic analysis of Sample No.6 excavated from Stratum IIIc. The metallographic sample was extracted from the marked location. $b_1$: Macrostructure. $c_1$ and $c_2$: BE images of the area (Reg.1) in $b_1$ and the area (Reg.1-1) in $c_1$, respectively. (Excavation plan from Omura 2005)

the copper lump, and the copper slag (Tables 5 and 6).

Inductively coupled plasma optical emission spectroscopy (ICP-OES), using a PERKIN ELMER Optima 4300DV, was employed for the chemical analysis of fifteen elements (except for sultur) from the iron objects (indicating in Tables 2 and 3) and twenty three elements (except for sultur) from the copper objects (indicated in Tables 4 and 7). The elements determined, and the analytical lines selected (nm), were as follows: Fe (238. 204), Cu (324. 752), Ni (231. 604), Co (228. 616), Mn (257, 610), P (213, 617), Ti (334. 940), Si (251. 611), Ca (393. 366), Al (396. 153), Mg (285. 213), V (290. 880), As (193. 696), Mo (202. 031), Cr (284. 325), Sn (189. 927), Pb (220. 353), Zn (206. 200), Sb (206. 836), Bi (223. 061), Ag (338. 289), Au (267. 595), W (207. 912), Ba (233. 527). Sulfur content in Samples No.5 to No.9 was tested by the infrared absorption method (IRA) after combustion in a current of oxygen, using a LECO CS444.This was the same method that was used with Sample No.3. (Akanuma 2003) Subsamples from No.5 to No.9 used for chemical analysis had their external corrosion layers removed with a diamond-coated wheel to avoid contamination from burial deposits.

In order to prevent evaporation of Si, a new preparation method was employed for this research. Approximately fifty milligrams of the dried surface subsamples (Nos.1 through 4) and inner subsamples (No.5, No.7, No.8 and No.9) for Si analysis were weighed in a TMF vessel; 3.033ml of HCl (30wt %) and 0.763ml of $HNO_3$ (65 wt%) and 3.033ml of twice distilled water was then added to the subsumples. The closed vessel was put into a microwave oven, using a PERKIN ELMER MULTIWAVE B30MCO3A,

Table 1 Examined objects from Stratum IIIc and Stratum IIIb-IIIc

| No. | Object | Description of Excavation | | | | | | Year Number | Stratum |
|---|---|---|---|---|---|---|---|---|---|
| | | Sector | | Grid | Date | Provisional Layer | Structure | | |
| 1 | Iron Fragment | North | XXIV | XLVIII-56 | 940805 | ⑬ | - | - | IIIc |
| 2 | Iron Fragment | North | XII | XLIX-54 | 940727 | ⑬ | R150 | - | |
| 3 | Iron Fragment | North | XII | XLIX-55 | 940714 | ⑫ | R150 | - | |
| 4 | Iron Fragment | North | XII | XLIX-55 | 940714 | ⑫ | R150 | - | |
| 5 | Iron Slag | North | IV | XXXVIII-55 | 920711 | ㊶ | - | - | |
| 6 | Copper Lump | North | III | XL-55 | 920710 | ㊼ | - | - | IIIc |
| 7 | Copper Slag | North | V | XXXVII-55 | 060726 | ㊼ | P2954 | 06000488 | |
| 8 | Copper Slag | North | VII | XXXII-54 | 060920 | ㊹ | - | 06000349 | IIIb-IIIc |
| 9 | Copper Slag | North | VIII | XXXI-55 | 060808 | ㊾ | P2968 | 06000487 | IIIc |

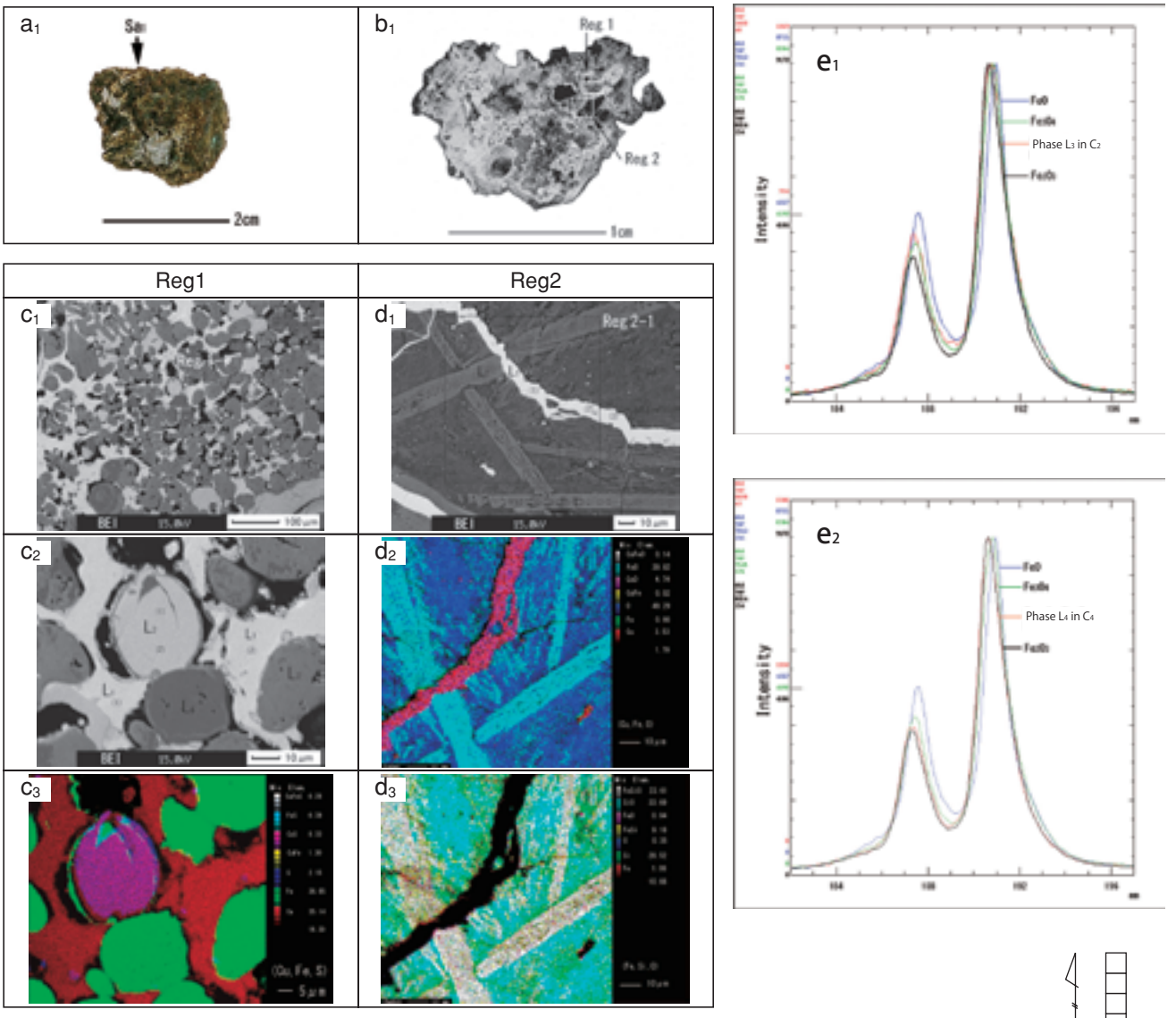


Fig. 4. Metallographic analysis of Sample No.7 excavated from Stratum IIIc. $a_1$: External appearance. The metallographic sample was extracted from the marked location. $b_1$: Macrostructure. $c_1$ and $c_2$: BE images of the area (Reg.1) in $b_1$ and the area (Reg.1-1) in $c_1$, respectively. Fig.$c_3$: Combined X-ray color-map of Cu-Kα, Fe-Kα, and S-Kα of $c_2$. $d_1$: BE image of the area Reg.2 in $b_1$. $d_2$ and $d_3$: Combined X-ray color maps of Cu-Kα, Fe-Kα, and O-Kα, and Fe-Kα, Si-Kα, and O-Kα within the area (Reg.2-1) in $d_1$, respectively. The phase $L_1$ in $d_1$ is believed to be cuprite and the phase $L_2$ in $d_1$ is to be the compound of the Fe-Si-O system. $e_1$ and $e_2$: Fe-Lα and Fe-Lβ spectra of three Fe standard samples (FeO, $Fe_3O_4$, and $Fe_2O_3$), and the phase $L_3$ and the phase $L_4$ in $c_2$ by EPMA. The predominant constituents of phase $L_3$ and phase $L_4$ are believed to be magnetite and hematite, respectively. (Excavation plan from Omura 2005)

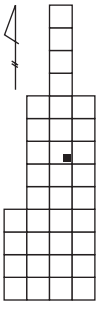

Table 2 Composition of iron artifacts from Stratum IIIc by ICP-OES, IRA, and EPMA

| No. | Sub No. | chemical components (mass%) | | | | | | | | | | | | | | | element ratios: Co, Cu, Ni | | | | m.s. | n.m.i. |
|---|---|---|---|---|---|---|---|---|---|---|---|---|---|---|---|---|---|---|---|---|---|---|
| | | T.Fe | Cu | Ni | Co | Mn | P | Ti | Si | Ca | Al | Mg | V | As | Mo | S | Co*(Co/Ni) | Cu*(Cu/Ni) | Ni**(Ni/Co) | Cu**(Cu/Co) | | |
| 1 | $Sa_1$ | 59.54 | 0.062 | 0.013 | 0.011 | 0.013 | 0.04 | 0.013 | 1.35 | 0.493 | 0.128 | 0.168 | - | - | - | - | 0.85 | 4.77 | 1.18 | 5.64 | Cm (0.1-0.2) | no |
| | Suf | 30.65 | 0.007 | 0.005 | 0.003 | 0.047 | 1.35 | 0.180 | 13.8 | 1.64 | 2.26 | 0.442 | 0.080 | 0.15 | 0.003 | - | - | - | - | - | - | - |
| 2 | $Sa_1$ | 51.47 | 0.002 | 0.002 | 0.001 | 0.010 | 0.21 | 0.099 | 4.55 | 0.445 | 1.32 | 0.240 | <0.001 | <0.01 | <0.001 | - | - | - | - | - | no | Wus, Gl |
| | Suf | 25.99 | 0.003 | 0.003 | 0.002 | 0.040 | 1.25 | 0.256 | 14.5 | 1.78 | 3.26 | 0.719 | 0.071 | 0.28 | 0.018 | - | - | - | - | - | - | - |
| 3 | $Sa_1$ | 70.52 | 0.082 | 0.002 | 0.006 | 0.004 | 0.06 | 0.003 | 0.76 | 0.052 | 0.067 | 0.030 | <0.001 | <0.01 | <0.001 | 0.21 | - | - | 0.33 | 13.7 | Cm (0.1-0.3) | Gl, Po |
| | Suf | 15.94 | 0.004 | 0.004 | 0.001 | 0.103 | 0.90 | 0.256 | 17.8 | 3.43 | 5.07 | 0.858 | 0.068 | 0.27 | 0.005 | - | - | - | - | - | - | - |
| 4 | $Sa_1$ | 69.36 | 0.041 | 0.003 | 0.007 | 0.007 | 0.11 | 0.004 | 0.83 | 0.337 | 0.104 | 0.049 | <0.001 | <0.01 | <0.001 | - | - | - | 0.43 | 5.86 | Cm (0.2-0.3) | no |
| | Suf | 22.77 | 0.004 | 0.003 | 0.001 | 0.057 | 1.30 | 0.137 | 12.6 | 3.54 | 3.24 | 0.772 | 0.065 | 0.32 | 0.008 | - | - | - | - | - | - | - |

Suf = sample extracted from the outer surface of the iron artifact
$Sa_1$ = sample extracted from inner portion of the iron artifact
Cm = cementite or its holes; the numbers in parentheses are carbon contents estimated from microstructure
m.s. = micro structure
n.m.i. = non-metallic inclusions

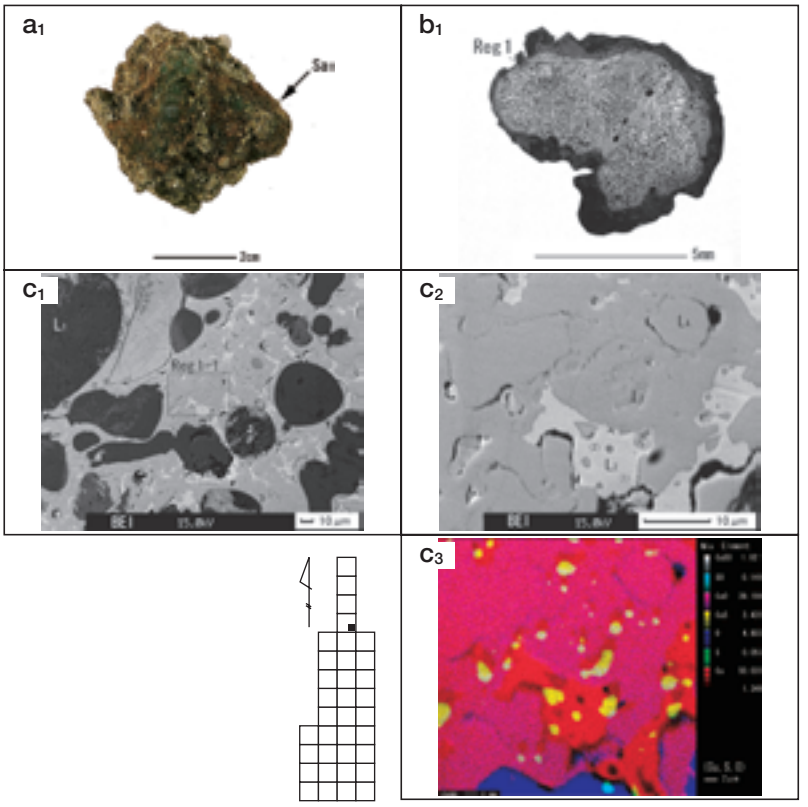


Fig. 5. Metallographic analysis of Sample No.8 excavated from Stratum IIIb-IIIc. $a_1$: External appearances. The metallographic sample was extracted from the marked location. $b_1$: Macrostructure. $c_1$ and $c_2$: BE images of the area (Reg.1) in $b_1$ and the area (Reg.1-1) in $c_1$, respectively. $c_3$: Combined X-ray color-map of Cu-Kα, S-Kα, and O-Kα of $c_2$. (Excavation plan from Omura 2005)

operating at a frequency of 2450MHz, and a three stage program was started (first stage: 100-400W, time 5 min; second stage: 600W, 5min; third stage: 1000W, 20min). After cooling to room temperature, 0.625ml of HF (40 wt%) was added to the subsamples and then dissolved overnight. 12ml of boric acid (4 wt%) was added to the subsamples. The sample solution was transferred into polypropylene bottles and made into 50ml total volume solutions with twice-distilled water. ICP-OES was used to determine Si contents in Tables 2, 4, and 7. All the reagents used were Merck Suprapur chemicals. The analytical methods for other elements used here were the same as in a previous paper (Akanuma 2001), with the exception of those used for the copper lump, Sample No.6.

The sample from No.6, a copper lump, was washed with ethyl alcohol and acetone, and dried for three hours at 110 °C. 20 mg of the sample was weighed in a Teflon vessel. 0.5 ml of HCl and 0.25 ml of $HNO_3$ were added to the sample, and then dissolved over night. The resultant solution was diluted with ultra pure water to yield a solution containing 1 mg of sample per milliliter (Hirao et al. 1992). ICP-OES was also used to determine the seventeen elements (all except sulfur) in Table 4.

## 5. ANALYTICAL RESULTS

### 5.1 Chemical composition of iron artifacts and iron slag

Table 2 shows the analytical data obtained by ICP-OES for the iron objects. The total iron content (T.Fe) of each of the four inner subsamples was less than 71 mass%. This indicates that the inner samples of the iron artifacts were composed mainly of iron corrosion. These corroded samples must have undergone migration and loss of main and trace elements, and contamination of trace elements from the surrounding soil. It is very difficult to estimate

Table 3 Chemical composition of iron slag from Stratum IIIc by ICP-OES and IRA

| No. | Sub. No | T.Fe | Cu | Ni | Co | Mn | P | Ti | Si | Ca | Al | Mg | V | As | Mo | Cr | S |
|---|---|---|---|---|---|---|---|---|---|---|---|---|---|---|---|---|---|
| 5 | $Sa_1$ | 37.52 | <0.001 | 0.048 | 0.018 | 0.099 | 0.41 | 0.057 | 5.65 | 4.22 | 0.938 | 0.642 | 0.010 | - | 0.014 | 0.003 | - |
| | $Sa_1$(n) | 15.26 | 0.010 | 0.007 | 0.005 | 0.144 | 1.00 | 0.067 | 12.5 | 9.74 | 2.20 | 0.823 | 0.024 | 0.16 | 0.005 | 0.003 | 0.09 |

Table 4 Chemical composition of a copper lump by ICP-OES

| No. | Cu | Sn | Pb | Zn | As | Sb | Bi | Fe | Ni | Ag | Au | Co | Mn | Al | Ti | W | Mo | S |
|---|---|---|---|---|---|---|---|---|---|---|---|---|---|---|---|---|---|---|
| 6 | 87.4 | 0.04 | 0.913 | 0.184 | 0.75 | 0.36 | <0.01 | 4.06 | 0.064 | 0.02 | 0.03 | 0.031 | <0.001 | 0.008 | <0.001 | 0.001 | 0.201 | 1.17 |

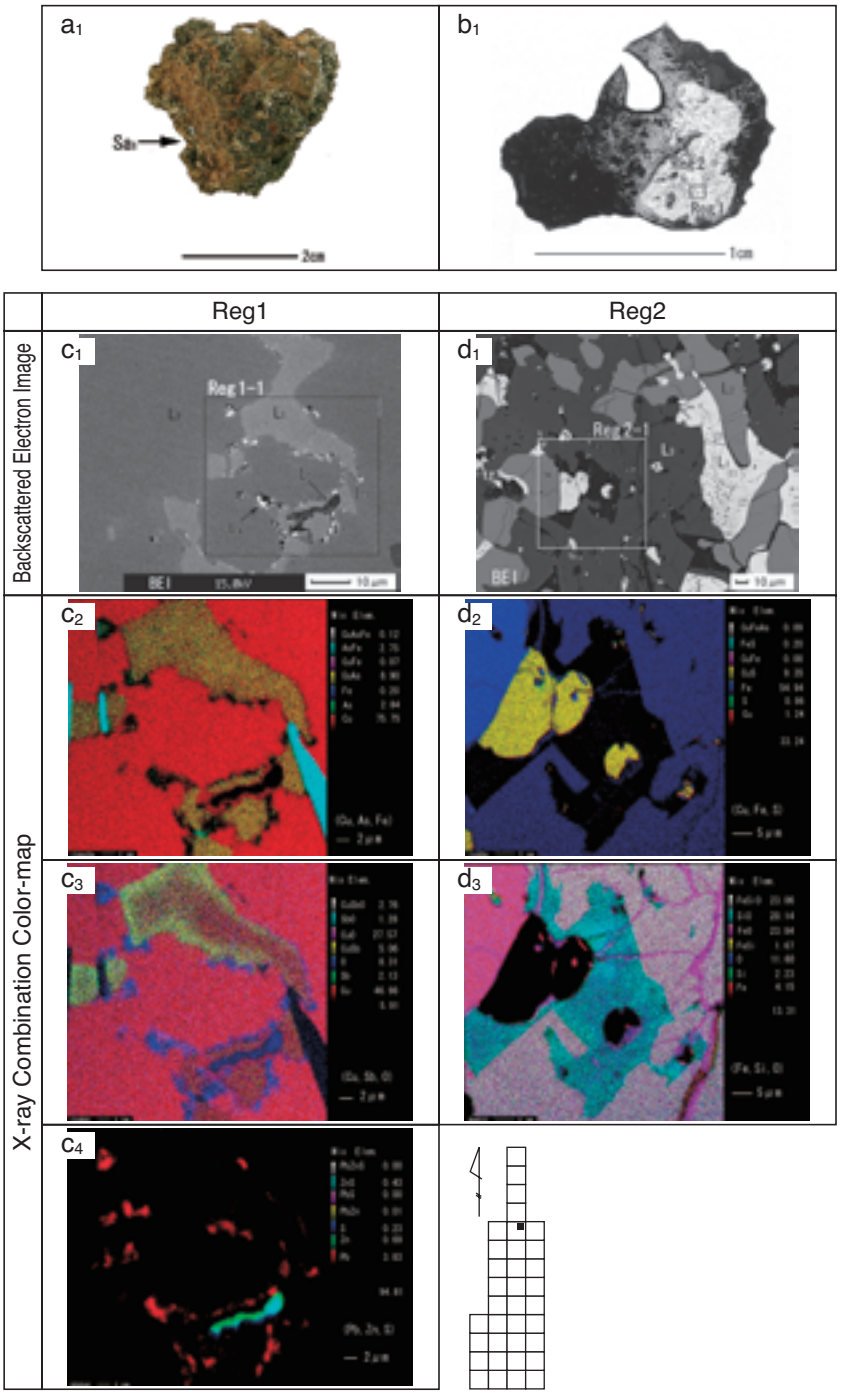


Fig. 6. Metallographic analysis of Sample No.9 excavated from Stratum IIIc. $a_1$: External appearance. The metallographic sample was extracted from the marked location. $b_1$: Macrostructure. $c_1$: BE image of the area (Reg.1) in $b_1$. $c_1$ to $c_3$: Combined X-ray color-maps of Cu-Kα, As-Lα, and Fe-Kα, Cu-Kα, Sb-Lα, and O-Kα, and Pb-Mα, Zn-Kα, and S-Kα of the area (Reg.1-1) in $c_1$, respectively. $d_1$: BE image of the area (Reg.2) in $b_1$. $d_2$ and $d_3$: Combined X-ray color-maps of Cu-Kα, Fe-Kα, and S-Kα, and Fe-Kα, Si-Kα, and O-Kα of the area (Reg.2-1) in $c_1$, respectively. (Excavation plan from Omura 2005)

the influence of migration and loss phenomena upon the original chemical compositions in each sample. Therefore, we should consider the possibility of contamination of trace elements from the surrounding soil before discussing each analytical result first. Then, we need to pay attention to the trace elements believed to have almost the same chemical behavior in the corroding process and minimal influence by burial deposits.

As discussed in a previous paper (Akanuma 2005), the elements Cu, Ni, and Co are believed to remain in the iron metal throughout the process of smelting, refining, and forging. If there is little contamination from the burial deposits by Ni, Co, and Cu, these three elements can be used as characteristics for classifying the iron artifacts or iron lumps. Fig. $1a_1$ shows the Cu, Ni, and Co concentrations detected in the four inner samples ($Sa_1$) and the four surface samples (Suf) extracted from Samples No.1 to No.4. We believe the concentrations of Cu, Ni, and Co contained in Samples No.1, No.2, and No.4 originated from the objects themselves, [2] specifically from the raw iron materials used to make them. In Sample No.3, it is difficult to judge the influence of burial contaminants, but when the trace element content in the inner samples is less than 0.005mass%, that influence is believed to be negligible.

Fig. $1b_1$ shows the Mn, P, Ti, and As concentrations. The values of Mn, P, Ti, and As in the four surface samples are higher than those in the inner sample of each corresponding sample. It is difficult to classify iron artifacts by using only the contents of these four elements (As, Mn, P, and Ti), because

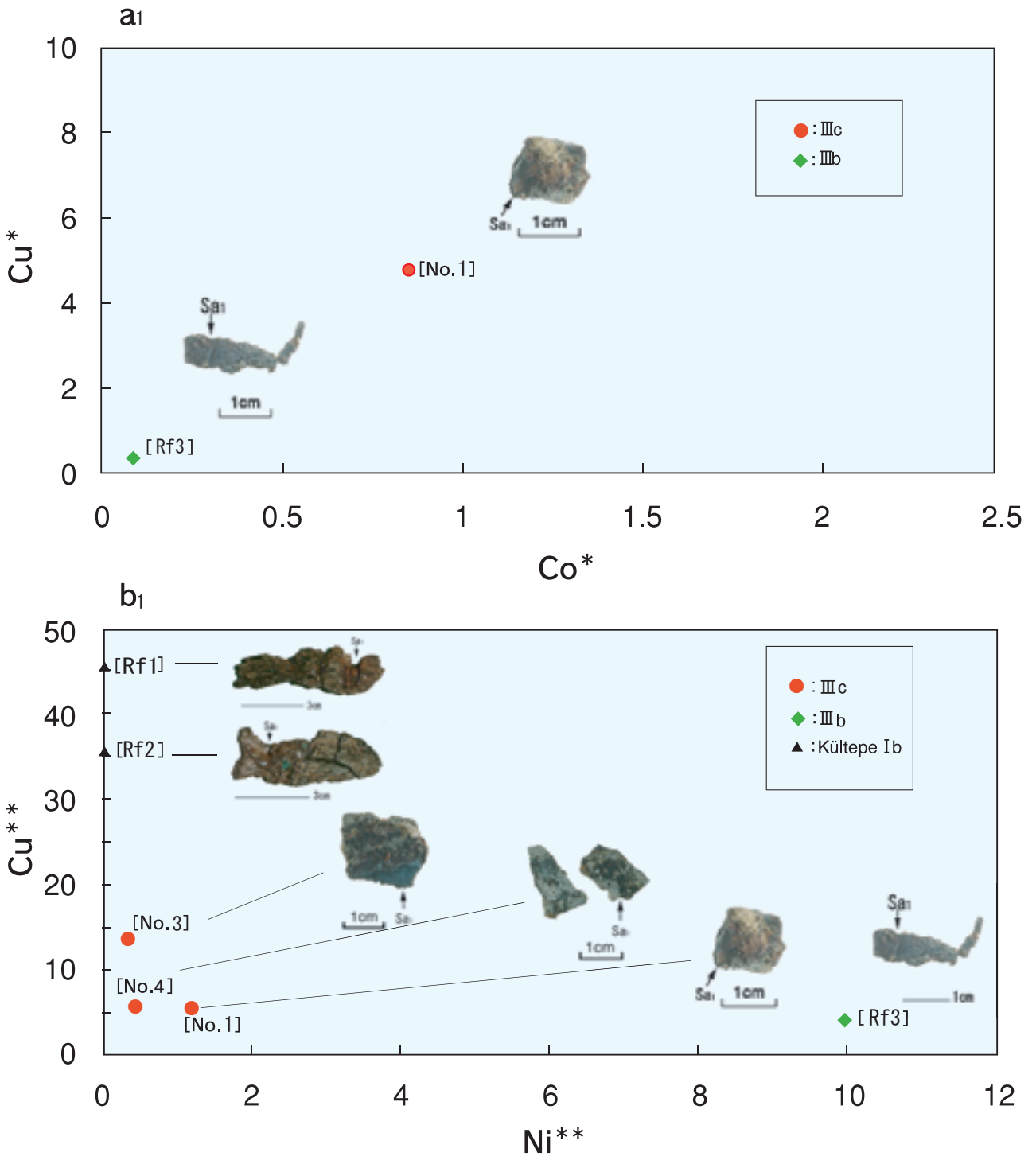


Fig. 7. Relationship between Co* {the values of (mass% Co)/(mass% Ni)} and Cu* {the values of (mass% Cu)/(mass% Ni)} and between Ni** {the values of (mass% Ni)/(mass% Co)} and Cu** {the values of (mass% Cu)/(mass% Co)} in the iron objects excavated from Stratum IIIc. The plots with numbers are analytical results in this paper. Rf1 and Rf2 (black triangles ▲) are the samples from Kültepe Karum Ib level, and Rf3 (green diamonds ◆) is a sample from Stratum IIIb.

Table 5 Results of quantitave analysis of copper slag by EPMA

| No. | Spot | | | chemical components (mass %) | | | | | | | | | | | | total |
|---|---|---|---|---|---|---|---|---|---|---|---|---|---|---|---|---|
| | | | | Cu | Fe | As | Sb | Pb | Mo | Ag | Ni | Co | Ca | S | Cl | O | |
| 6 | Reg1 in Fig.3c$_1$ | $L_1$ | - | 96.5 | 3.13 | - | <0.01 | <0.01 | <0.01 | <0.01 | <0.01 | - | <0.01 | 0.01 | 0.01 | 0.03 | 99.68 |
| | | $L_2$ | (1) | 86.4 | 1.74 | - | <0.01 | <0.01 | <0.01 | <0.01 | <0.01 | - | <0.01 | <0.01 | 0.16 | 10.8 | 99.10 |
| | | | (2) | 86.2 | 1.12 | - | <0.01 | <0.01 | <0.01 | <0.01 | <0.01 | - | <0.01 | 0.01 | 0.29 | 10.4 | 98.02 |
| 7 | Reg1 in Fig.4c$_2$ | $L_1$ | (1) | 90.3 | 5.44 | 1.33 | - | - | - | - | - | 0.01 | - | 0.11 | - | 0.82 | 98.01 |
| | | | (2) | 90.8 | 5.21 | 1.55 | - | - | - | - | - | 0.03 | - | 0.12 | - | 0.75 | 98.46 |
| | | $L_2$ | (1) | 75.9 | 3.64 | - | - | - | - | - | - | - | - | 19.3 | - | - | 98.84 |
| | | | (2) | 75.2 | 3.96 | - | - | - | - | - | - | - | - | 19.3 | - | - | 98.46 |
| 8 | Reg1 in Fig.5c$_2$ | $L_2$ | (1) | 93.0 | 3.22 | 0.74 | <0.01 | <0.01 | <0.01 | <0.01 | <0.01 | <0.01 | <0.01 | <0.01 | <0.01 | 0.45 | 97.41 |
| | | | (2) | 91.9 | 2.78 | 2.33 | <0.01 | <0.01 | <0.01 | <0.01 | <0.01 | <0.01 | <0.01 | <0.01 | <0.01 | 0.44 | 97.45 |
| 9 | Reg2 in Fig.6d$_1$ | $L_1$ | (1) | 77.4 | 1.97 | - | - | - | - | - | - | - | - | 19.0 | - | 0.32 | 98.69 |
| | | | (2) | 75.5 | 2.07 | - | - | - | - | - | - | - | - | 19.0 | - | 0.49 | 97.06 |
| | | | (3) | 75.6 | 1.96 | - | - | - | - | - | - | - | - | 18.8 | - | 0.42 | 96.78 |

Table 6 Results of quantitative analysis of the bright phase ($L_1$) found in the area (Reg.2) in Sample No.7 by EPMA

| Spot $L_1$ | chemical components (mass %) | | | | total |
|---|---|---|---|---|---|
| | $Cu_2O$ | FeO | MnO | $SO_3$ | |
| (1) | 98.50 | 2.44 | <0.01 | 0.01 | 100.95 |
| (2) | 98.24 | 2.20 | <0.01 | 0.01 | 100.45 |
| (3) | 98.28 | 2.15 | <0.01 | 0.03 | 100.46 |

there is a strong possibility of contamination of those four elements from the surrounding soil.

The surface portions of Samples No.1 to No.4 have an As content exceeding 0.1 mass%. The same phenomenon was observed in samples excavated from North Sector XXIX-XXX in 2000 (Akanuma 2003), North Sectors XIX, XX, and XXVI in 2001 (Akanuma 2004), and North Sectors X, XVI, XVIII, and XIX and South Sector LVI in 2004 (Akanuma 2006). Considering that several objects related to copper production activity were discovered in Stratum II and III levels (Masubuchi and Nakai 2005), it is believed that high As contents originate from soil pollution associated with this activity. This should be clarified by further research.

[2] We can assume the concentrations of three elements in Sample No.2 originate from the object itself. This assumption is based on the comparison to the concentration of three elements in Sample No.4 which is not as corroded as Sample No.2. The same argument was stated in previous papers (Akanuma 2005).

Sample No.5Sa$_1$(n) has a 15.26 mass% T.Fe. The other main components are Si, Ca, Al, and P (each equal to or above 1.00 mass%). This indicates that the new subsample extracted from this lump is composed mainly of iron slag. The previous analysis of this object yielded 37.52 mass% T.Fe, 0.048 mass% Ni, and 0.018 mass% Co, all higher than in the reanalysis. As shown in the metallographic result, Sample No.5 is composed of iron slag and iron corrosion. It is certain that a major difference in the above-mentioned analyses resulted from the heterogeneity of Sample No.5.

## 5.2 Metallographic examination of iron slag

Sample No.5 is a small lump of dark brown slag (Fig. 2a$_1$). Fig. 2b$_1$ shows the cross-section of this sample. The structure consists of iron corrosion (gray-white or gray area) and iron slag (dark gray area), and voids and cracks. In the EPMA backscattered electron (BE) image of the region (Reg.1) in Fig. 2b$_1$, fine crystals (Cm) with a metallic luster and fine dark structures are observed (Fig. 2c$_1$). The EPMA combined X-ray color-map reveals that the main components of these white crystals are Fe and C (Fig. 2c$_2$). The fine white crystals are believed to be cementite.[3] The fine dark structures are believed to be holes formed by loss of the fine white crystals, because a secondary electron (SE) image and an elemental distribution map by EPMA made it clear that these areas were composed of epoxy resin.

Minute iron Particles and an area composed of iron

Table 7 Composition of copper slag by ICP-OES and IRA

| No. | Sub No. | chemical components (mass%) | | | | | | | | | | | | | | | | | | |
|---|---|---|---|---|---|---|---|---|---|---|---|---|---|---|---|---|---|---|---|---|
| | | T.Fe | Cu | Ni | Co | Mn | P | Ti | Si | Ca | Al | Mg | V | Pb | As | Mo | Sb | Bi | Ba | S |
| 7 | $Sa_1$ | 27.55 | 44.8 | 0.021 | 0.088 | 0.002 | <0.01 | 0.028 | 3.31 | <0.01 | 0.289 | 0.083 | 0.001 | 0.069 | 0.65 | 0.010 | 0.03 | <0.01 | 0.203 | 2.31 |
| 8 | $Sa_1$ | 22.51 | 56.1 | 0.031 | 0.032 | 0.008 | <0.01 | 0.009 | 0.12 | 0.085 | 0.074 | 0.040 | 0.002 | 0.179 | 5.38 | 0.040 | 0.16 | <0.01 | 0.005 | 1.17 |
| 9 | $Sa_1$ | 26.65 | 50.3 | 0.039 | 0.067 | 0.006 | <0.01 | 0.006 | 0.22 | 0.082 | 0.051 | 0.025 | 0.008 | 0.068 | 0.51 | 0.007 | 0.01 | <0.01 | 0.005 | 2.37 |

oxide ($L_1$ in Fig. $2d_1$) are embedded in the dark gray area ($L_2$ in Fig. $2d_1$) and the dark area ($L_3$ in Fig. $2d_1$). Both of the areas $L_2$ and $L_3$ are composed mainly of $K_2O$, $Al_2O_3$, and $SiO_2$ (Figs. $2d_2$ and $2d_3$). The contents of $K_2O$ and $Al_2O_3$ in area $L_2$ are higher than in area $L_3$ (Fig. $2d_3$).

## 5.3 Chemical composition of lumps of copper and copper slag

Sample No.6 is a small copper lump weighing approximately 2.5 g (Fig. $3a_1$). The sample contains 87.4 mass% Cu, 4.06 mass% Fe, 1.17 mass% S, 0.913 mass% Pb, 0.75 mass% As, and 0.36 mass% Sb (Table 4). The contents of Fe and S above 1 mass% are believed to originate from residual iron oxide or sulfuric compounds.

The chemical composition of the three lumps of copper slag, Nos. 7 to 9, is given in Table 7. The data indicate that for all copper slag the main components are Cu, iron oxide, and S. The T.Fe and Cu contents vary widely from 22 to 28 mass% and 44 to 57 mass%, respectively. The element As occurs as a trace element (<0.7 mass%) in Samples No.7 and No.9, but in Sample No.8 is 5.38 mass % — i.e., is a main component. It is believed that this result is mainly derived from a Cu- and Fe-based alloy found in the microstructure of Sample No.8. The Si content of Sample No.7 is higher in Samples No.8 and No.9; this indicates that slag composed of a large amount of $SiO_2$ coexists with the metallic phases. This is consistent with the result of the metallographic examination.

## 5.4 Metallographic examination of the copper lump and copper slag

Fig. $3b_1$ is a macrostructure of Sample No.6 (Fig.$3a_1$). A gray area and a dark gray area coexist in this structure. Fig. $3c_1$ is an BE image of the area (Reg.1) in Fig. $3b_1$. According to the EPMA quantitative analyses (Table 5), the gray phase ($L_1$ in Fig. $3c_1$) consists mainly of copper containing 3.13 mass% Fe and the dark gray phases ($L_2$(1) and $L_2$(2) in Fig. $3c_1$) are almost the same as cuprite containing 1 to 2 mass% Fe {$(Cu,Fe)_2O$}. The bright area ($L_3$) in Fig. $3c_1$ is composed mainly of an inclusion of the Pb-Cu-Mo-O system. There are a light gray area ($L_4$) and a gray phases ($L_5$) embedded in copper containing 1 to 2 mass% of Fe in the area (Reg.1-1) in Fig. $3c_1$. EPMA analyses revealed that the area $L_4$ was an inclusion of the Pb-Cu-O system and the phase $L_5$ was a Cu-Sb-based alloy (Fig. $3c_2$).

Sample No.7 (Fig. $4a_1$) is a dark brown copper slag covered by a lot of soil and weighing approximately 2.5 g. This slag has weak magnetism. The macrostructure of the extracted sample has many voids and cracks (Fig. $4b_1$). BE images of the area (Reg.1) in Fig. $4b_1$ and the area (Reg.1-1) in Fig.$4c_1$ show that it consists mainly of four phases {bright phase ($L_1$), light gray phase ($L_2$), gray phase ($L_3$), and dark gray phase ($L_4$)} (Figs. $4c_1$ and $4c_2$). The EPMA quantitative analyses (Table 5) and the combined X-ray color-map of Cu-Kα, Fe-Kα, and S-Kα (Fig. $4c_3$) reveal that phase $L_1$ is composed mainly of copper containing 5 to 6 mass% Fe and 1 to 2 mass% As, and phase $L_2$ copper sulfide (believed to be chalcocite containing above 3 mass% Fe {Cc: $(Cu,Fe)_2S$}). Figs. $4e_1$ and $4e_2$ show the Fe-Lα line and Fe-Lβ line spectra of three Fe standard samples (FeO, $Fe_3O_4$, and $Fe_2O_3$), and phase $L_3$ and phase $L_4$ in Fig. $4c_2$.The peakshape of phase $L_3$ is almost the same as that of $Fe_3O_4$, and the peakshape of phase $L_4$ is almost the same as that of

[3] Similar white crystals found in a dagger were identified as cementite in an archaeometallurgical analysis of the crystals (Knox 1963).

$Fe_2O_3$. Therefore, the predominant constituent of phase $L_3$ is believed to be magnetite and that of phase $L_4$ to be hematite. In the area (Reg.2) in Fig. $4b_1$, the bright phase ($L_1$) and the gray skeletal phase ($L_2$) in a glassy area including minute compounds are observed (Fig. $4d_1$). The streaks and striations of phase $L_1$ are very clear. This phase is believed to be cuprite containing 2 to 3 mass% FeO {$(Cu, Fe)_2O$}. Phase $L_2$ is a compound of the Fe-Si-O system. These results are based on the data in Table 6 and the combined X-ray color-maps (Figs. $4d_2$ and $4d_3$).

The macrostructure of Sample No.8 (Fig. $5a_1$) is composed mainly of three phases (Fig. $5b_1$). The backscattered electron image of phase $L_1$ in the area (Reg.1) in Fig. $5b_1$ is iron oxide (see discussion of phases $L_3$ and $L_4$ in Sample No.7 above). Phase $L_2$ in the area (Reg.1-1) in Fig. $5c_1$ (Fig. $5c_2$) consists of copper containing 2 to 4 mass% Fe and 0.7 to 3 mass% As (Table 5). Phases $L_3$ and $L_4$ in Fig. $5c_2$ are an area of the Cu-S system and an area of the Cu-O system, respectively, based on the combined X-ray color-map of Fig. $5c_2$ (Fig. $5c_3$).

In the macrostructure of Sample No.9 (Fig. $6a_1$), a light gray area, a gray area, and a dark gray area coexist (Fig. $6b_1$). The backscattered electron image of the area (Reg.1) in the light gray area (in Fig.$6b_1$) consists mainly of a Cu-As-Sb alloy (gray phase $L_1$), a Cu-As-Pb-Sb alloy (dark gray phase $L_2$), and a Fe-As alloy (gray phase $L_3$). In addition, bright minute inclusions of the Pb-Sb-O system ($L_4$) and dark inclusions ($L_5$) are present in the grain boundaries of the above-mentioned three phases. On the other hand, in the area (Reg.2) in Fig. $6b_1$, a light gray phase ($L_1$) almost completely composed of copper sulfide {believed to be chalcocite containing approximately 2 mass% Fe; [Cc:$(Cu,Fe)_2S$]} and a gray phase ($L_2$: iron oxide containing Zn) can be seen. These phases $L_1$ and $L_2$ are surrounded by the dark gray phase ($L_3$) which consists mainly of Fe, Si, and O and a dark glassy area. These analytical results are based on the data in Table 5 and EPMA combined X-ray color-maps (Figs. $6c_2$ to $6c_4$, $6d_2$, and $6d_3$). Samples No.8 and No.9 also have weak magnetism in common with Sample No.7.

## 6. DISCUSSION

### 6.1 Production activity related to iron during the Assyrian Colony Period at Kaman-Kalehöyük

The results of the metallographic analysis of iron samples No.1 to No.4 were discussed in previous papers (Akanuma 2002; 2003). The summarized results are expressed in Table 2. It was ascertained that Samples No.1, No.3, and No.4 were made of steel whose carbon content is estimated from the microstructure to be 0.1 mass% to 0.3 mass%. Sample No.2 was made of artificially produced iron; however, no structures identified as steel were found in this sample because of its advanced state of corrosion. Precipitates consisting mainly of Fe and S {believed to be pyrrhotite (Po; $Fe_{1-x}S$) based on the result of EPMA analysis} were found in Sample No.3 (Akanuma 2003). This indicates that sulfur compounds may have been contained in the iron ore used.

Iron slag, which reflects production activities related to iron, was found in a structure dating to the Assyrian Colony Period (Sample No.5). The microstructure of this slag indicates that it solidified after being in a state where partially or completely melted slag was in contact with metallic iron partially consisting of steel.

At least three manufacturing processes are needed to make steel: smelting, refining, and forging. However, it is difficult to identify the manufacturing process by which Sample No.5 was produced. According to Dr. Sachihiro Omura, several pieces of iron slag were discovered from a structure dating to the Assyrian Colony Period during the 2007 excavation season. We will be able to understand the actual conditions of the iron producing activities at Kaman-Kalehöyök during the Assyrian Colony Period more clearly by analyzing these objects. In addition, based on the discovery of iron slag from the structure dating to the Assyrian Colony Period, we can consider the possibility that iron production methods had already been established during the cultural age of Stratum IV. This matter should be clarified by gathering further information about iron objects from Stratum IV, and by performing archaeometallurgical analysis on those objects.

### 6.2 Composition of iron fragments from Stratum IIIc

As stated in a previous paper (Akanuma 2005), even if the same raw iron materials are used to make iron as a starting material, different manufacturing methods and production conditions can produce a difference in the chemical composition of the final iron product. Therefore, it is not useful to classify archaeological objects by direct comparison of chemical compositions. As discussed in Section 5.1, contamination from the surrounding soil is another factor affecting chemical composition of the materials.

Except for desulfurization and several novel processes developed recently, the refining of iron and steel has involved a preferential oxidation of impure elements. As already mentioned, the elements Cu, Ni, and Co are believed to remain in the iron metal throughout the process of smelting, refining, and forging: it can be easily concluded by thermodynamics that Fe should be oxidized prior to these three elements.[4] Also, there is little contamination from the burial deposits by Ni, Co, and Cu. Therefore, the concentration ratios of these three elements in the archeological objects should be similar to those in the raw materials used to produce the objects if no additional alloying was carried out. The values of (mass% Co)/(mass% Ni) (called here Co*) and (mass% Cu)/(mass% Ni) (Cu*) were calculated for the iron artifacts which contain more than 0.005 mass% Ni. In addition, the values of (mass% Ni)/(mass% Co) (Ni**) and (mass% Cu)/(mass% Co) (Cu**) were calculated for the samples containing more than 0.005 mass% Co. The calculated results are listed in Table 2.

The relationship between (mass% Co)/(mass% Ni) and (mass% Cu)/(mass% Ni) in the archaeological iron objects dating to the Assyrian Colony Period from Kaman-Kalehöyük is indicated on Fig. $7a_1$, and the relationship between (mass%Ni)/(mass%Co) and (mass%Cu)/(mass%Co) is indicated on Fig. $7b_1$. In Fig. $7b_1$, two iron fragments from Kültepe Karum Ib level (Rf1 and Rf2) (Akanuma 2003) and an iron fragment from Stratum IIIb at Kaman-Kalehöyük (Rf3) (Akanuma 2005) are also plotted. Sample No.2 is not plotted in Figs. $7a_1$ and $7b_1$ because of its low contents of Ni and Co, and Samples No.3, No.4, Rf1, and Rf2 are not plotted in Fig.$7a_1$ because of the low Ni contents (under 0.005 mass%) or high values of Cu* (above 890).

The element ratio data support the probability that there was more than one supply source of iron objects (raw materials, smelted iron materials, smelted and refined iron materials, or manufactured iron artifacts as final products) during the Assyrian Colony Period and the Old Hittite Kingdom Period. Also, the supplying districts of iron objects to Kaman-Kalehöyük in the Assyrian Colony Period were different from those to Kültepe, as indicated by a very clear difference in trace element compositions between the materials from Kaman-Kalehöyük and Kültepe. It is understood that the pre-Hittite residents (the so-called "proto-Hittites") at Kaman-Kalehöyük had adopted the advanced culture of Mesopotamia, based on excavation results. For example, red-polished earthenware with Mesopotamian characteristics was excavated from an Assyrian Colony Period structure.[5] Many objects brought from Mesopotamia have been discovered at the site of Kültepe (Özgüç 1986). This archaeological evidence indicates that central Anatolia had strong commercial links with Mesopotamia.

Therefore, three possibilities can be considered in relation to the acquisition of iron objects and the techniques of iron production at Kaman-Kalehöyük. First, the proto-Hittites developed iron production techniques independently. Second, iron objects or iron producing techniques were brought from the Mesopotamian district by the Assyrians or another people.[6] Third, iron production techniques were established through cooperation between the proto-Hittites and the Assyrians, or another people, and then iron objects were produced at or near Kaman-Kalehöyük. Considering that iron slag was identified in a Stratum

[4] Thermodynamic calculation by Prof. Kimihisa Ito, Department of Science and Engineering, Waseda University.

[5] Private communication by Dr.Sachihiro Omura.

[6] According to Dr. Masako Omura, it is almost certain that Anatolian merchants performed commercial activities in central Anatolia as well as Assyrian merchants. This is based on research findings related to seals and stamp seals.

IIIc structure and that there is a clear difference in trace element compositions between Kaman-Kalehöyük and Kültepe objects, as mentioned in Section 6.2, the author believes that the archaeological objects excavated from Stratum IVa (the level below IIIc) are a key to understanding this matter.

### 6.3 Production activity related to copper during the Assyrian Colony Period at Kaman-Kalehöyük

Copper lump Sample No.6 is composed mainly of copper containing approximately 4 mass% of Fe, cuprite, and a small amount of lead oxide inclusions. It is regarded as an object without utility value because it contained a considerable amount of impurities. Samples No.7, No.8, and No.9 are extremely heterogeneous slag consisting mainly of copper containing a small amount of iron, copper sulfide, and iron oxide. EPMA analysis revealed that copper sulfide and iron oxide found in Sample No.7 may be chalcocite containing above 3 mass% Fe {$(Cu,Fe)_2S$}, magnetite, and hematite. This result indicates that copper sulfide ores (such as chalcopyrite) were used to obtain copper during the Assyrian Colony Period at Kaman-Kalehöyük or in surrounding areas.

In general, copper ores are classified into two main types: oxide and sulfide. Oxide ores are reduced with carbon in the form of charcoal, and then copper is extracted from oxide ores. On the other hand, sulfide ores usually contain several kinds of impurities. It is necessary to remove these impurities, especially iron (II) sulfide ($Fe_{1-X}S$), known as one of the major impurities in the process of copper making.

The traditional copper sulfide smelting process is as follows. First, the sulfide ores are concentrated and roasted. As a result, considerable amounts of sulfur are eliminated as sulfur oxides, and copper is concentrated in the inner portions of the ores. Second, mineralized material obtained after roasting is smelted in the furnace in order to produce a copper-iron sulfide mixture. In this process, the roasted ores coexist with charcoal, whose role is to supply a high enough temperature and to produce a reducing atmosphere for production of that mixture. Two types of slag are produced during this operation. One is furnace slag, which remains in the furnace, and the other is tap slag, which flows out of the furnace (Tumiati *et al*. 2005). These two types of slag usually include a small amount of charcoal, various partially reacted materials, minerals, and metal. Third, the obtained copper-iron sulfide mixture is melted again and converted to crude copper by smelting (airing or adding copper oxide). In this process, the iron in the copper-iron sulfide mixture is oxidized and wüstite (FeO) is produced, which reacts with silicates in slag and then is removed from copper to slag as fayalite ($Fe_2SiO_4$). Chalcocite ($Cu_2S$) and cuprite ($Cu_2O$) are produced with the procession of the oxidative reaction of the copper-iron sulfide mixture. Finally crude copper is produced by the reaction of these two compounds or oxidation of chalcocite by oxygen in the air. Magnetite is also formed by the oxidation of wüstite.[7)]

It is very difficult to ascertain the production methods or stages from which Samples No.7, No.8, and No.9 came. It is not clear that a roasting process was used during the Assyrian Colony Period at Kaman-Kalehöyük or surrounding areas. Considering these samples have almost the same metal alloys and mineral compounds as those produced in the process of the oxidative reaction of a copper-iron sulfide mixture, the author believes that they are a product of this process.[8)] This matter should be clarified by additional research.

A clear difference in the chemical composition in the three lumps of copper slag was recognized. This indicates that copper ore or smelted copper may have been brought to Kaman-Kalehöyük from multiple regions during the period spanning Stratum IIIc to Stratum IIIb. Considering that the lead isotope ratio between lead

---

7) The hematite found in Sample No.7 is estimated to be a byproduct of the oxidation of magnetite.

8) The following method is presented as the simplest method of smelting sulfide ores (Prentiss 1980). First sulfide ore is roasted in order to convert copper sulfide to copper oxide and sulfur oxide, iron sulfide to iron oxide and sulfur oxide. The resultant copper oxide is reduced in the furnace. Finally copper metal is obtained. However, it is very difficult to extract only copper oxide from sulfide ore by roasting. Moreover, it is not possible to explain the metal and mineral compounds found in Samples No.7, No.8, and No.9 (these compounds are almost the same products as those produced by the oxidative reaction of a copper-iron sulfide mixture), based on the above-mentioned process. Therefore the author could not conclude that Samples No.7, No.8, and No.9 were produced in this simple method.

objects from Stratum IIIb and Stratum IVa are quite similar (Hirao *et al*. 1992; Enomoto and Hirao 2006), we will be able to approach a better understanding of the change from bronze to iron in the Near East by further examination of copper and iron objects excavated from Stratum IIIb, IIIc, and IVa at Kaman-Kalehöyük.

## 7. CONCLUSION

An archaeometallurgical analysis was undertaken to clarify the composition of five iron objects and four copper objects dating to the Assyrian Colony Period. As a result, five issues were clarified.

1. Iron slag was found in a structure dating to the Assyrian Colony Period at Kaman-Kalehöyük. The composition of this slag indicated that some kind of iron producing activity in which metallic iron contacted with melted or partially melted slag.

2. There was a difference in trace element compositions among three iron fragments from Kaman-Kalehöyük, and between Kaman-Kalehöyük and Kültepe. This indicates that there was more than one supply source for iron objects (raw materials, smelted iron materials, smelted and refined iron materials, or manufactured iron artifacts as final products) to Kaman-Kalehöyük.

3. It is almost certain that copper sulfide ores (such as chalcopyrite) were used to obtain copper during the Assyrian Colony Period at Kaman-Kalehöyük or surrounding areas.

4. There is a high possibility that crude copper was produced by using a copper-iron sulfide mixture at Kaman-Kalehöyük.

5. By performing further archaeometallurgical analysis on the excavated iron and copper objects from Stratum IIIb, IIIc, and IVa at Kaman-Kalehöyük, and from other contemporary archaeological sites in central Anatolia, we will be able to gain a better understanding of the actual conditions relating to the transition from copper to iron production in the Near East.

## ACKNOWLEDGEMENTS

The author is very grateful to Dr. Sachihiro Omura and all the members of the Kaman-Kalehöyük excavation team for their support of this study and useful suggestions. The author also appreciates the helpful comments of Dr. Kimihisa Ito, Dr. Nobutaka Tsuchiya, Ms. Claire Peachey, and Mr. Kyle Steinke.

## BIBLIOGRAPHY

Akanuma, H.

1995a "Metallurgical Analysis of Iron Artifacts and Slag Excavated from Kaman-Kalehöyük," *AAS* IV, pp.119-133 (in Japanese).

1995b "Metallurgical analysis of Iron Artifacts and Slag from Archaeological Site of Kaman-Kalehöyük," *BMECCJ* VIII, pp.59-88.

2001 "Iron Objects from Stratum II at Kaman-Kalehöyük: Correlation between Composition and Archaeological Levels," *AAS* IIX, pp.217-288.

2002 "Iron Objects from the Architectural Remains of Stratum III and Stratum II at Kaman-Kalehöyük: Composition and Archaeological Levels," *AAS* XI, pp.191-200.

2003 "Further Archaeometallurgical Study of 2nd and 1st Millennium BC Iron Objects from Kaman-Kalehöyük," *AAS* XII, pp.137-149.

2004 "Archaeometallurgical Analysis of Iron and Copper Objects from Stratum III and Stratum II at Kaman-Kalehöyük: Correlation between Composition and Archaeological Levels," *AAS* XIII, p.163-174.

2005 "The Significance of the Composition of Excavated Iron Fragments from Stratum III at the Site of Kaman-Kalehöyük, Turkey," *AAS* XIV, pp.147-157.

2006 "Changes in Iron Use during the 2nd and 1st Millennia B.C. at Kaman-Kalehöyük, Turkey: Composition of Iron Artifacts from Stratum III and Stratum II," *AAS* XV, pp.207-222.

Enomoto, J. and Hirao, Y.

2006 "Lead Isotope Ratios of Lead Objects Excavated from Kaman- Kalehöyük," AAS XV,pp.223-247.

Hirao, Y., M. Sasaki, M. Takenka and T. Uchida

1992 "Lead isotope study of copper objects excavated from Kaman-Kalehöyük," *AAS* I, pp.165-186.

Knox, R.

1963 "Detection of Carbide Structure in the Oxide Remains of Ancient Steel," *Archaeometry* 6, pp.43-45.

Masubuchi, M. and I. Nakai

2005 "Scientific Analysis of Metallurgical Slag Excavated from Kaman-Kalehöyük (1)," *AAS* XIV, pp.183-194.

Özgüç, T.

1986 "New Observations on the Relationship of Kültepe with Southeast Anatolia and North Syria during the Third Millennium B.C.," in J. V. Canby *et al*. (eds), *Ancient Anatolia: Aspects of Change and Cultural Development*, Wisconsin Studies in Classics, pp.31-47.

Tumiati, S. Casartelli, P., Mambretti, A., and Martin, S.

2005 "The ancient mine of Serviette (Saint-Marcle, Vol d'Aosta, western Italian Alps): a mineralogical, metallurgical and charcoal analysis of furnace slags," *Archaeometry* 47(2), pp.317-340.

Prentiss S. de Jesus

1980 "The development of prehistoric mining and metallurgy in Anatolia," *British Archaeological Reports*, International Series 74 (i), pp.27-29.

***Hideio Akanuma***
***Iwate Prefectural Museum***
***34 Uedamatsuyashiki, Morioka***
***Iwate 020-0102***
***Japan***
***Akamuma@iwapmus.jp***